

Physics-Informed Neural Networks for Solving Two-Flavor Neutrino Oscillations in Vacuum and Matter Environments for Atmospheric and Reactor Neutrinos

T. Srinivasan*

Department of Physics, School of Advanced Sciences, Vellore Institute of Technology, Chennai, India

Kalyani Desikan†

Department of Mathematics, School of Advanced Sciences, Vellore Institute of Technology, Chennai, India

(Dated: May 14, 2026)

Neutrino oscillations provide crucial insights into fundamental particle physics, with two-flavor approximations effectively describing reactor and atmospheric phenomena. This paper investigates the application of Physics-Informed Neural Networks (PINNs), which have several advantages over traditional solvers. Traditional methods typically depend on mesh-based techniques or dimensionality reduction approaches to solve the governing differential equations for neutrino evolution in vacuum and matter environments. We review the theoretical framework, including vacuum mixing and the Mikheyev–Smirnov–Wolfenstein (MSW) effect in matter, and demonstrate PINN implementations for vacuum and constant-density profiles. This Machine learning based approach for reactor (low-energy) and atmospheric (high-energy) neutrinos shows high precision similar to analytical solutions, with mean squared errors of the order of 10^{-3} – 10^{-4} . We have also discussed the robustness of PINNs in solving coupled ODE systems, along with future extensions to three-flavor effects.

I. INTRODUCTION

Neutrinos, elusive particles with tiny masses, exhibit flavor oscillations due to quantum mixing between mass eigenstates, a phenomenon confirmed by experiments such as Super-Kamiokande (atmospheric) [1] and the Sudbury Neutrino Observatory (SNO) (solar) [2]. Although the three-flavor framework provides the most complete description, the two-flavor approximation remains a robust and essential tool for understanding dominant oscillation channels [3], such as those observed in solar, atmospheric and reactor neutrino experiments [4–6].

In the two-flavor picture, one typically considers the $\nu_e \leftrightarrow \nu_\mu$ (or $\nu_e \leftrightarrow \nu_\tau$) system driven by the solar mass splitting $\Delta m_{21}^2 \sim 7.5 \times 10^{-5} \text{ eV}^2$ and mixing angle $\theta_{12} \simeq 34^\circ$, or the $\nu_\mu \leftrightarrow \nu_\tau$ system driven by the atmospheric mass splitting $\Delta m_{32}^2 \sim 2.5 \times 10^{-3} \text{ eV}^2$ and mixing angle $\theta_{23} \simeq 45^\circ$ [7–9].

Reactor antineutrinos are produced as a byproduct of the nuclear fission process in a nuclear reactor. In a typical pressurized water reactor (PWR) or boiling water reactor (BWR), energy is generated primarily through thermal neutron-induced fission of four primary isotopes: ^{235}U , ^{238}U , ^{239}Pu , and ^{241}Pu [10].

When these heavy nuclei undergo fission, they split into two lighter, neutron-rich fission fragments. To reach the valley of beta stability, these unstable fragments undergo a series of beta decays (β^-), emitting an electron and an electron antineutrino in the process.

$${}^A_Z X \rightarrow {}^A_{Z+1} Y + e^- + \bar{\nu}_e \quad (1)$$

The energy of these antineutrinos typically ranges from 0 to about 10 – 12 MeV [3], peaks at approximately 2 MeV. Reactor neutrino experiments have provided precise measurements of the mixing angle θ_{13} and confirmed the three-flavor oscillation paradigm [6, 11, 12]. These results are consistent with solar and atmospheric neutrino observations [1, 2]. Reactor neutrinos offer a precise and controlled probe of neutrino mixing parameters in the vacuum regime. And they play a crucial role in completing the global picture of neutrino oscillations [13].

Atmospheric neutrinos are generated when high-energy cosmic rays collide with air nuclei [14, 15], in the atmosphere of the earth producing pions (π^\pm) and kaons (K^\pm) that decay into muons (μ^\pm) and neutrinos (ν^\pm). Atmospheric neutrino oscillations are driven predominantly by the atmospheric mass-squared splitting and near-maximal mixing and cover an immense range of baselines L and energies E : neutrinos can be observed from directly overhead ($L \sim 15 \text{ km}$) to trajectories through the Earth’s diameter ($L \sim 1.2 \times 10^4 \text{ km}$), with energies from sub-GeV to TeV scales [16]. Unlike reactor neutrinos, atmospheric neutrinos can traverse Earth, experiencing matter effects in the mantle and core compared to the former. Determining precise oscillation probabilities through these dense environments is crucial to determine the ordering of the neutrino mass [17, 18].

Traditional numerical methods, such as Runge–Kutta (RK4) or finite difference schemes [19], have long been the standard for solving neutrino evolution equations. Although effective for constant densities, these mesh-based (NOTE: A traditional computational technique such as Finite Difference or Finite Element methods used to solve differential equations by discretizing a continuous physical domain—like space or time—into a structured grid, or “mesh,” of individual points.) approaches face significant challenges when applied to re-

* srinivasan.t2022@vitstudent.ac.in

† kalyanidesikan@vit.ac.in

alistic, highly variable density profiles like the Preliminary Reference Earth Model (PREM) [20]. Often requiring adaptive step-sizes and complex interpolation[21] to maintain stability near density discontinuities (e.g., the core-mantle boundary). Furthermore, they operate as “black boxes,” making inverse problems such as inferring oscillation parameters from data computationally expensive [22].

In contrast, Physics-Informed Neural Networks (PINNs) [23] represent a paradigm shift in computational physics. This Machine Learning based approach[24] offers a promising method for solving the evolution equations of neutrino oscillations by incorporating physical constraints directly into neural network training, achieving high accuracy by eliminating computational mesh requirements. Unlike traditional purely data-driven approaches, PINNs integrate fundamental physical laws encoded as partial differential equations (PDEs) directly into the neural network loss function, enabling a very close approximation to achieve accurate solution even in data-sparse regimes. This paradigm shift represents a significant departure from conventional numerical methods such as finite element methods (FEM) and finite difference methods (FDM)[25, 26], which rely on explicit mesh generation and suffer from computational overhead in high-dimensional problems. The PINN framework achieves physics consistency by the PDEs as soft constraints through residual loss terms, thereby regularizing the learned solution and preventing overfitting to noisy measurements. This approach has proven highly effective in fields ranging from fluid dynamics [27, 28] to quantum mechanics [25, 29]. The primary advantage of PINNs lies in their flexibility, particularly their ability to evaluate governing equations at randomly sampled continuous points, entirely bypassing the computational bottleneck of generating discrete grids for variable density profiles. Furthermore, PINNs seamlessly facilitate data assimilation by embedding empirical measurements—such as observed survival probabilities from neutrino detectors—directly into the network’s loss function alongside the physical constraints. This architecture naturally allows the simultaneous solution of forward and inverse problems [26, 30]. Although PINNs have been successfully applied to fluid dynamics and classical mechanics, their application to quantum unitary evolution in high-energy physics remains underexplored. This paper presents a new approach to PINNs in the domain of neutrino phenomenology. Unlike previous general-purpose solvers, we particularly design a complex-valued network architecture specifically tailored to preserve the unitarity of the neutrino evolution operator. In addition, since standard deep neural networks only output real numbers, the PINN cannot directly output a single complex number. So, we split the complex Schrödinger equation into its real and imaginary components here.

The remainder of this paper is organized as follows.

In Section II, we review the theoretical formalism of two-flavor neutrino oscillations, detailing the quantum mechanical propagation dynamics in both vacuum and constant matter environments. Section III presents the Methodology of the proposed Physics-Informed Neural Network (PINN), including the network architecture, the treatment of the complex Schrödinger equation, and the construction of the physics-informed loss function. In Section IV, we present our numerical results and discuss the performance of the PINN framework in accurately capturing the survival and appearance probabilities for both solar and atmospheric neutrino configurations. Finally, Section V concludes the paper and outlines potential directions for future research.

II. THE FORMALISM OF NEUTRINO OSCILLATIONS

In this Section, we outline the two-flavor neutrino oscillations in vacuum and constant matter environments by detailing the mathematical formalisms for its propagation. The latter of which introduces the crucial Mikheyev–Smirnov–Wolfenstein (MSW) effect.

A. Two-flavor oscillations in vacuum

The neutrino flavor eigenstates $|\nu_\alpha\rangle$ ($\alpha = e, \mu$) are related to the mass eigenstates $|\nu_i\rangle$ ($i = 1, 2$) via a unitary mixing matrix [31],

$$\begin{pmatrix} |\nu_e\rangle \\ |\nu_\mu\rangle \end{pmatrix} = \begin{pmatrix} \cos\theta & \sin\theta \\ -\sin\theta & \cos\theta \end{pmatrix} \begin{pmatrix} |\nu_1\rangle \\ |\nu_2\rangle \end{pmatrix}, \quad (2)$$

where θ is the vacuum mixing angle and $\Delta m^2 = m_2^2 - m_1^2$ is the mass-squared difference between the mass eigenstates ν_2 and ν_1 . In the ultra-relativistic limit, the time evolution of the mass eigenstates is governed by a Schrödinger-like equation,

$$i \frac{d}{dt} |\nu_i(t)\rangle = E_i |\nu_i(t)\rangle, \quad (3)$$

with $E_i \approx p + m_i^2/(2E)$, where p and E are the momentum and the energy of the neutrinos. In flavor space, the evolution can be written as

$$i \frac{d}{dt} |\nu_i(t)\rangle = E_i |\nu_i(t)\rangle, \quad (4)$$

with $E_i \approx p + m_i^2/(2E)$, where p and E are the momentum and the energy of the neutrinos. In flavor space, the evolution can be written as

$$i \frac{d}{dt} \begin{pmatrix} \nu_e(t) \\ \nu_\mu(t) \end{pmatrix} = H_F \begin{pmatrix} \nu_e(t) \\ \nu_\mu(t) \end{pmatrix}, \quad (5)$$

where $x \approx t$ for ultra-relativistic neutrinos, $H_F = UM^2U^\dagger$ with

$$U_M = \begin{pmatrix} \cos\theta_M & \sin\theta_M \\ -\sin\theta_M & \cos\theta_M \end{pmatrix}, \quad (6)$$

and the state being

$$\psi(t) = \begin{pmatrix} \nu_e(t) \\ \nu_\mu(t) \end{pmatrix}, \quad (7)$$

then the effective Hamiltonian in the flavor basis is given by the equation;

$$H_F = \frac{\Delta m^2}{4E} \begin{pmatrix} -\cos 2\theta & \sin 2\theta \\ \sin 2\theta & \cos 2\theta \end{pmatrix}. \quad (8)$$

By substituting the effective Hamiltonian matrix H_F in the time evolution equation for the two flavor neutrino oscillation in terms of the mixing angle is given as [3];

$$i \frac{d}{dx} \begin{pmatrix} \psi_{ee} \\ \psi_{e\mu} \end{pmatrix} = \frac{1}{4E} \begin{pmatrix} -\Delta m^2 \cos 2\theta & \Delta m^2 \sin 2\theta \\ \Delta m^2 \sin 2\theta & \Delta m^2 \cos 2\theta \end{pmatrix} \begin{pmatrix} \psi_{ee} \\ \psi_{e\mu} \end{pmatrix}. \quad (9)$$

Let us assume the flavor of neutrino that is produced is ν_e at $x = 0$. Then the initial conditions are given by

$$\Psi_e(0) = \begin{pmatrix} \psi_{ee}(0) \\ \psi_{e\mu}(0) \end{pmatrix} = \begin{pmatrix} 1 \\ 0 \end{pmatrix}. \quad (10)$$

Now, the appearance and survival probabilities at baseline L be found using the relations;

$$P_{e\mu}^{\text{vac}}(L) = |\psi_{e\mu}(x)|^2, \quad (11)$$

$$P_{ee}^{\text{vac}}(L) = |\psi_{ee}(x)|^2 = 1 - P_{e\mu}^{\text{vac}}(L) \quad (12)$$

The analytical solution for the evolution equation is then given by the transition probabilities;

$$P_{ee}^{\text{vac}}(L) = 1 - \sin^2 2\theta \sin^2 \left(\frac{\Delta m^2 L}{4E} \right), \quad (13)$$

$$P_{e\mu}^{\text{vac}}(L) = \sin^2 2\theta \sin^2 \left(\frac{\Delta m^2 L}{4E} \right). \quad (14)$$

These probabilities depend on the ratio L/E , leading to the characteristic oscillatory behavior used in experimental analyses.

B. Two-flavor oscillations in matter

When neutrinos propagate through matter, the coherent forward scattering of ν_e on electrons via charged-current interactions introduces an effective potential [32]

$$V_{CC} = \sqrt{2} G_F n_e, \quad (15)$$

where $G_F = 1.166 \times 10^{-5} \text{ GeV}^{-2}$ is the Fermi constant and n_e is the electron number density of the matter. For electrically neutral matter, neutral-current contributions are flavor-universal and can be dropped in the two-flavor approximation.

The effective Hamiltonian in matter becomes

$$H_{\text{mat}} = \frac{\Delta m^2}{4E} \begin{pmatrix} -\cos 2\theta & \sin 2\theta \\ \sin 2\theta & \cos 2\theta \end{pmatrix} + \begin{pmatrix} V_{CC} & 0 \\ 0 & 0 \end{pmatrix}. \quad (16)$$

For constant matter density, it is convenient to introduce the dimensionless parameter

$$Acc = \frac{2\sqrt{2} G_F n_e E}{\Delta m^2}, \quad (17)$$

where $n_e \simeq 3.65 \times 10^{27} \text{ m}^{-3}$. The effective mixing angle in matter θ_M and effective mass-squared difference Δm_M^2 become,

$$\sin^2 2\theta_M = \frac{\sin^2 2\theta}{(\cos 2\theta - Acc)^2 + \sin^2 2\theta}, \quad (18)$$

$$\Delta m_M^2 = \Delta m^2 \sqrt{(\cos 2\theta - Acc)^2 + \sin^2 2\theta}. \quad (19)$$

In our case study, we consider the constant matter density of the earth core ($\rho \approx 13 \text{ g/cm}^3$) for neutrinos to travel. The evolution equation of neutrinos to oscillate between two flavors in terms of the mixing angle in matter is given as [3]

$$i \frac{d}{dx} \begin{pmatrix} \psi_{ee} \\ \psi_{e\mu} \end{pmatrix} = \frac{1}{4E} \begin{pmatrix} -\Delta m_M^2 \cos 2\theta_M & \Delta m_M^2 \sin 2\theta_M \\ \Delta m_M^2 \sin 2\theta_M & \Delta m_M^2 \cos 2\theta_M \end{pmatrix} \begin{pmatrix} \psi_{ee} \\ \psi_{e\mu} \end{pmatrix}. \quad (20)$$

After performing the orthogonal transformation and diagonalising the effective Hamiltonian matrix H_{mat} the evolution equation becomes; $\Psi_e = U_M \Phi_e$.

If the matter-density is constant then the $d\theta_M/dx = 0$ and from the initial conditions we have

$$\begin{pmatrix} \phi_{e1}(0) \\ \phi_{e2}(0) \end{pmatrix} = \begin{pmatrix} \cos \theta_M & -\sin \theta_M \\ \sin \theta_M & \cos \theta_M \end{pmatrix} \begin{pmatrix} 1 \\ 0 \end{pmatrix} = \begin{pmatrix} \cos \theta_M \\ \sin \theta_M \end{pmatrix}. \quad (21)$$

The oscillation probabilities in constant matter density are then

$$P_{ee}^{\text{mat}}(L) = 1 - \sin^2 2\theta_M \sin^2 \left(\frac{\Delta m_M^2 L}{4E} \right) \quad (22)$$

$$P_{e\mu}^{\text{mat}}(L) = \sin^2 2\theta_M \sin^2 \left(\frac{\Delta m_M^2 L}{4E} \right). \quad (23)$$

For realistic propagation through the Earth or Sun, the density varies with position. In that case, $H(x)$ becomes explicitly position-dependent via $n_e(x)$, and the evolution equation must be solved with a space-dependent Hamiltonian, often using the PREM profile for Earth [20] or an exponential model for the Sun [33] respectively.

III. METHODOLOGY OF PHYSICS-INFORMED NEURAL NETWORKS

This section details our computational methodology used. We first describe the neural network architecture designed to output the real and imaginary components of the wavefunction. Then formulate the composite physics-informed loss function that rigorously enforces the Schrödinger equation based evolution and initial boundary conditions, and finally discuss the specific

implementations of the Hamiltonian for both vacuum and matter propagations.

A. Network architecture

We approximate the complex-valued neutrino wavefunction $\psi(x)$ using a fully connected feed-forward neural network. The primary input is the evolution parameter (baseline x or time t), and the outputs are the real and imaginary parts of the flavor amplitudes. For the two-flavor case, we write

$$\psi(x) = \begin{pmatrix} \psi_e(x) \\ \psi_\mu(x) \end{pmatrix} = \begin{pmatrix} \psi_e^{\text{Re}}(x) + i\psi_e^{\text{Im}}(x) \\ \psi_\mu^{\text{Re}}(x) + i\psi_\mu^{\text{Im}}(x) \end{pmatrix}, \quad (24)$$

and let the network output the four real components

$$\mathbf{u}(x) = (\psi_e^{\text{Re}}, \psi_e^{\text{Im}}, \psi_\mu^{\text{Re}}, \psi_\mu^{\text{Im}}). \quad (25)$$

A typical architecture used in our analyses consists of 6 hidden layers with 80–200 neurons per layer, employing hyperbolic tangent (tanh) activation function [34]. Training is carried out using gradient-descent based optimizers such as ADAM[35] and/or L-BFGS. ADAM is often employed in the early training stages for robust exploration of the parameter space, while L-BFGS can refine the solution and improve convergence near minima[36, 37]. The tanh activation function is preferred over ReLU[23, 38] for physics-informed problems due to its smoothness, allowing for the computation of higher-order derivatives required by the physics loss [39]. Weights are initialized using Glorot (Xavier) normal initialization to maintain stable gradients at the start of training.

B. Physics-informed loss function

The PINN is trained by minimizing a composite loss function $\mathcal{L}_{\text{total}}$ [23]:

$$\mathcal{L}_{\text{total}} = \mathcal{L}_{\text{ODE}} + \mathcal{L}_{\text{BC}}. \quad (26)$$

where \mathcal{L}_{ODE} enforces the evolution equation and normalization by means of probability conservation. \mathcal{L}_{BC} enforces the initial boundary conditions, such as the initial flavor state.

The evolution equation in vacuum or matter can be written generically as

$$i \frac{d}{dx} \psi(x) - H(x)\psi(x) = 0. \quad (27)$$

In practice, we split the real and imaginary parts. For example, in vacuum the flavor Hamiltonian is

$$H_{\text{vac}} = \frac{\Delta m^2}{4E} \begin{pmatrix} -\cos 2\theta & \sin 2\theta \\ \sin 2\theta & \cos 2\theta \end{pmatrix}, \quad (28)$$

and the corresponding real-imaginary system can be written as four coupled real equations for $\psi_e^{\text{Re}}, \psi_e^{\text{Im}}, \psi_\mu^{\text{Re}}$

and ψ_μ^{Im} . The residuals of these equations at collocation points $\{x_i\}$ define \mathcal{L}_{ODE} .

$$\mathcal{L}_{\text{ODE}} = \frac{1}{N_f} \sum_{i=1}^{N_f} \left\| i \frac{d\psi}{dx}(x_i) - \hat{H}\psi(x_i) \right\|^2. \quad (29)$$

Automatic differentiation (AD) [40], is used to compute spatial derivatives such as $d\psi_e^{\text{Re}}/dx$ exactly (to machine precision)[41], avoiding discretization error and maintaining a mesh-free formulation, and that the total probability is normalized throughout the evolution:

$$|\psi_e(x)|^2 + |\psi_\mu(x)|^2 = 1. \quad (30)$$

Normalization can be enforced either as a soft constraint in the loss or monitored as a diagnostic of training quality.

The boundary-condition loss \mathcal{L}_{BC} enforces that at the production point $x = 0$, the neutrino state is a pure flavor, for example

$$\psi_e(0) = 1, \quad \psi_\mu(0) = 0, \quad (31)$$

and is therefore defined as

$$\mathcal{L}_{\text{BC}} = \left\| \Psi_{\text{NN}}(0) - \begin{pmatrix} 1 \\ 0 \end{pmatrix} \right\|^2, \quad (32)$$

where $\Psi_{\text{NN}}(0)$ is the initial condition given by equation (10).

C. Implementation details

The main difference between vacuum and matter propagation in PINNs is Hamiltonian used in the residual. In vacuum, $H(x) = H_{\text{vac}}$ does not depend on matter density for fixed $\Delta m^2, E, \theta$. For constant matter density, we use

$$H_{\text{mat}} = H_{\text{vac}} + \begin{pmatrix} V_{\text{CC}} & 0 \\ 0 & 0 \end{pmatrix}, \quad (33)$$

with V_{CC} constant. The vacuum PINNs architecture for neutrinos oscillating in 2-flavors is thus given as in Fig. 1.

For spatially varying profiles, such as PREM for Earth [20] or an exponential solar profile, we use

$$H(x) = H_{\text{vac}} + V_{\text{CC}}(x), \quad (34)$$

with the electron density $n_e(x)$ given by the chosen model. The distinguishing feature for the matter case lies in the physics-informed loss function which forces the network to discover the non-linear amplitude enhancement and frequency shifts associated with the MSW effect. Figure 2 shows the PINNs architecture for the constant matter propagation of neutrinos oscillating in 2-flavors.

The network thus learns to approximate oscillations in both vacuum and matter once the analytic expressions for θ_M or Δm_M^2 are given; and after few trials and errors, these emerge from the differential equation.

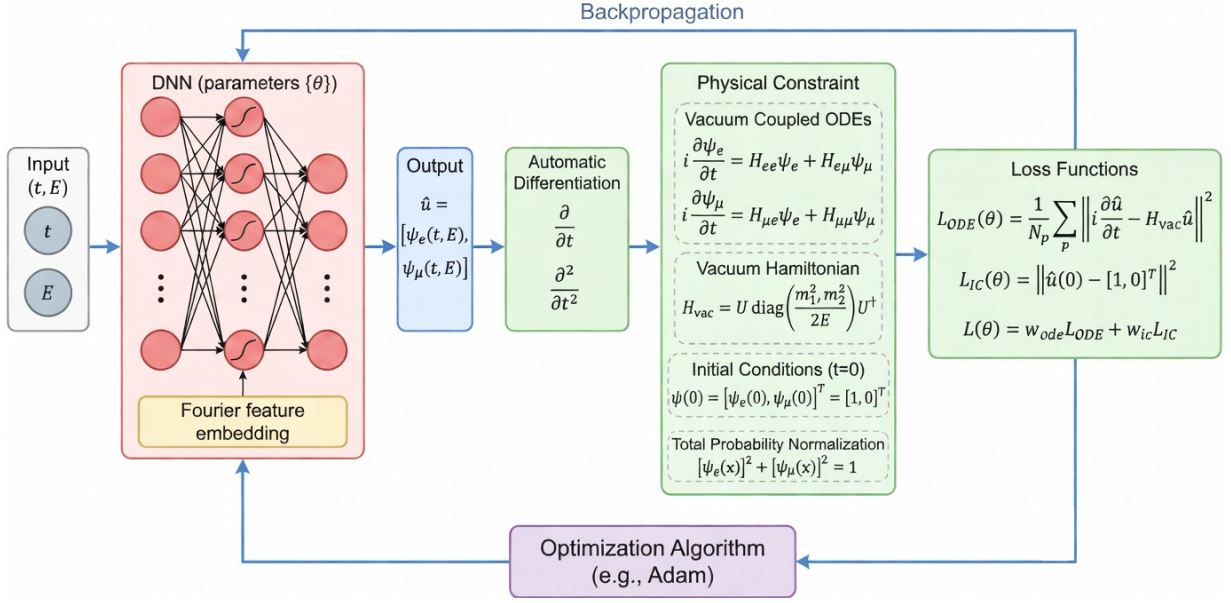


FIG. 1. PINNs architecture for neutrino propagation in vacuum.

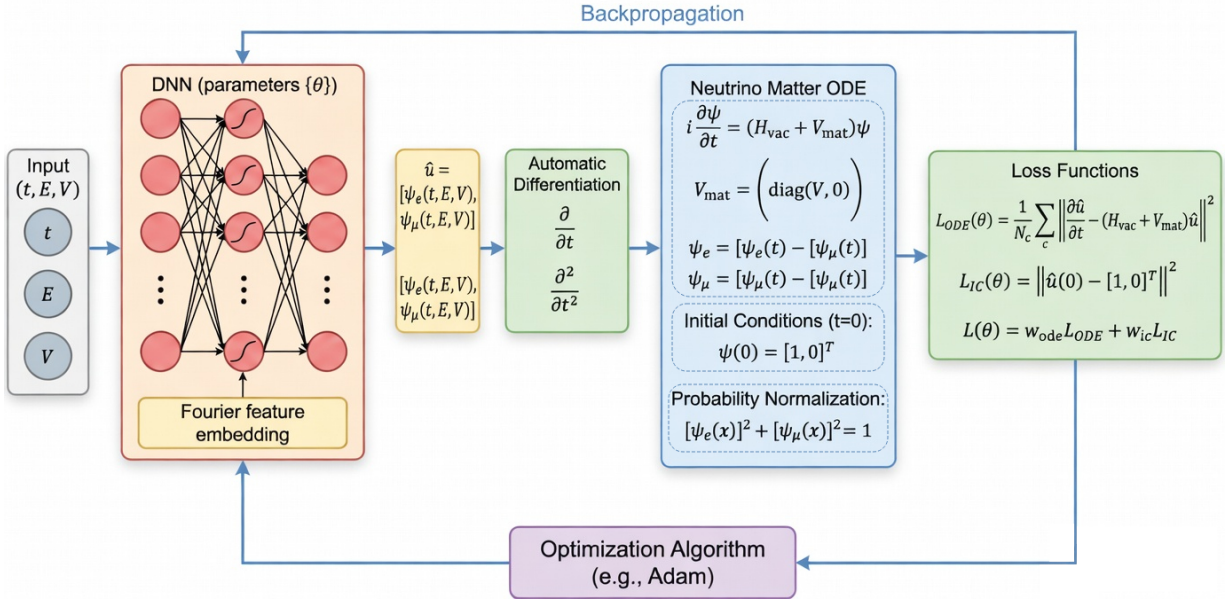


FIG. 2. PINNs architecture for neutrino propagation in matter.

IV. RESULTS AND DISCUSSION

In this section, we present the numerical solutions for two-flavor neutrino oscillations obtained using the Physics-Informed Neural Network (PINN) framework. We evaluate the network's performance for two distinct physical configurations: the **Reactor Neutrino** regime (low energy, small mass splitting) and the **Atmospheric Neutrino** regime (higher energy, larger mass splitting). For both cases, we compare the PINN predictions against the standard analytical solutions in vacuum and constant

matter environments.

A. Reactor Neutrino Configuration

The reactor neutrino oscillations were simulated using the characteristic parameters of the $\nu_e \rightarrow \nu_\mu$ channel: neutrino energy $E = 0.015$ GeV (15 MeV), solar mass-squared difference $\Delta m_{21}^2 = 7.5 \times 10^{-5}$ eV², and mixing angle $\theta_{12} = 33.4^\circ$.

1. Vacuum Propagation

The PINN was trained to solve the vacuum evolution equation over a baseline length L sufficient to capture the oscillation cycles. Fig. 3 compares the PINN-predicted survival probability $P(\nu_e \rightarrow \nu_e)$ and the appearance probability $P(\nu_e \rightarrow \nu_\mu)$ with the analytical vacuum formula, as given in equations (13) and (14)

The generated graph displays one of the smooth, repeating sinusoidal cycles of the survival and appearance probabilities over distance, cleanly plotted as continuous curves without discrete data points. The visualization excellently captures the expected quantum mechanical behavior: the appearance probability peaks at a maximum amplitude of roughly 0.85 (corresponding to the 33.4° mixing angle), with the mean squared error of around $1.4364\text{e-}03$ for survival and around $3.6170\text{e-}04$ for appearance probability, respectively.

2. Constant Matter Propagation (MSW Effect)

To investigate matter effects, we introduce a constant electron density potential V . The PINN solved the modified Schrödinger equation including the matter term. Despite the non-maximal vacuum mixing angle ($\theta = 33.4^\circ$), the matter potential modifies the effective mixing parameters. The generated graph in Fig. 4 presents the continuous, smooth curves for the survival and appearance probabilities, cleanly rendered without discrete data points with a mean squared error of around $1.2798\text{e-}03$ for survival and around $5.6455\text{e-}04$ for appearance probability, respectively. The PINN seamlessly captures this modified oscillatory behavior, accurately reflecting how the 33.4° mixing angle responds to the matter environment.

B. Atmospheric Neutrino Configuration

The atmospheric neutrino simulations were conducted using the $\nu_\mu \rightarrow \nu_\tau$ parameters: higher energy $E = 0.2$ GeV, larger atmospheric mass splitting $\Delta m_{32}^2 = 2.4 \times 10^{-3} \text{ eV}^2$, and maximal mixing angle $\theta_{23} = 45^\circ$.

1. Vacuum Propagation

In the atmospheric vacuum case, the oscillation is governed by near-maximal mixing ($\sin^2 2\theta \approx 1$). Figure 5 illustrates the survival and appearance probabilities for the same.

The PINNs seamlessly produces the survival and appearance probability graphs cleanly without any data points. The visualization closely mirrors the maximal amplitude (1.0) seen in the vacuum case, with the network accurately capturing the oscillation pattern along the wave continuously with the mean squared error

around $9.9762\text{e-}04$ for survival and around $9.0744\text{e-}04$ for appearance probability, respectively.

2. Constant Matter Propagation

In the case of matter, at $E = 0.2$ GeV, the matter potential V is relatively small compared to the vacuum term $\Delta m^2/2E$. Consequently, the matter effect is less pronounced than in the resonance region. The PINN effectively reproduces this behavior, generating a solution that deviates only slightly from the vacuum case, consistent with theoretical expectations for sub-GeV atmospheric neutrinos in standard earth densities with the mean squared error of around $3.0689\text{e-}04$ for survival and around $2.9586\text{e-}04$ for appearance probability, respectively as seen in Fig. 6.

The results confirm that the PINN architecture can handle the complex-valued coupled ODE system without numerical instability, provided the hyperparameters, particularly learning rate and iteration count, are tuned to mitigate spectral bias. The consistent achievement of MSE values in the order of $10^{-3}/10^{-4}$ across distinct energy scales and mixing regimes validates the robustness of the PINN architecture. Also indicating that the physics-informed loss function is sufficient to constrain the solution to the correct physical manifold, effectively handling both the maximal mixing of the atmospheric sector and the large-amplitude, non-maximal mixing of the reactor sector.

V. CONCLUSIONS AND OUTLOOK

We have demonstrated the efficacy of Physics-Informed Neural Networks as mesh-free solvers for two-flavor neutrino oscillations in vacuum, and constant matter density profiles. PINNs can reproduce oscillation probabilities with high accuracy, provided that the hyperparameters are carefully tuned to overcome spectral bias and resolve high-frequency phase information in the Schrödinger evolution.

This study serves as a proof-of-concept that deep learning frameworks can handle unitary quantum evolution and stiff gradients characteristic of neutrino phenomenology. Promising directions for future work include:

Extending the architecture to the full three-flavor framework, including the PMNS matrix and CP-violating phase δ_{CP} , and resolving both solar Δm_{21}^2 and atmospheric Δm_{31}^2 scales simultaneously.

ACKNOWLEDGMENTS

This research is supported by the Department of Science and Technology (DST), India, under the Fund for Improvement of S&T Infrastructure in Universities and Higher Educational Institutions (FIST) Program [Grant

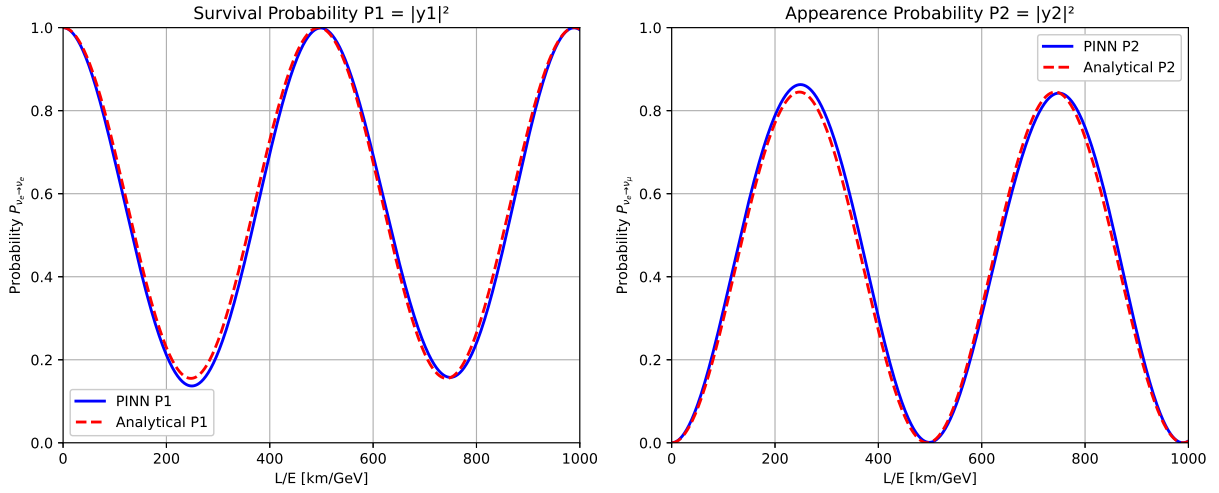


FIG. 3. Survival and Appearance Probability of Reactor neutrino in vacuum case

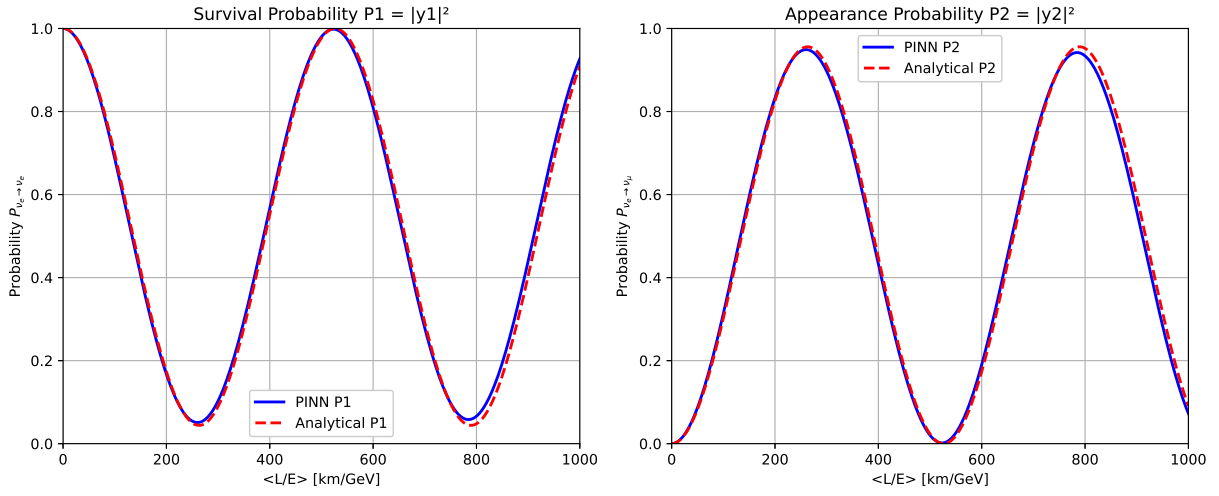


FIG. 4. Survival and Appearance Probability of Reactor neutrino in constant matter case

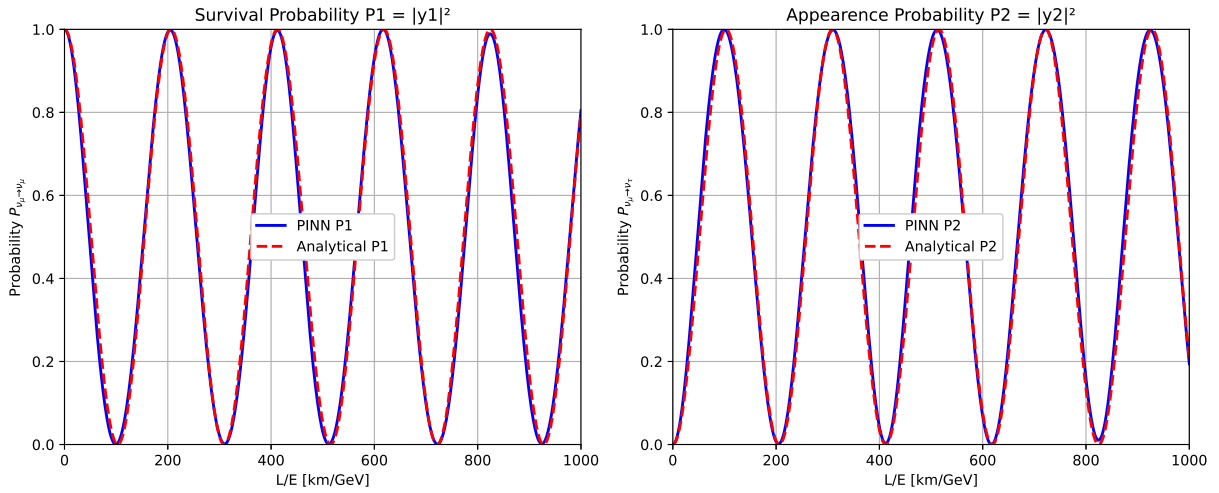


FIG. 5. Survival and Appearance Probability of Atmospheric neutrino in vacuum case

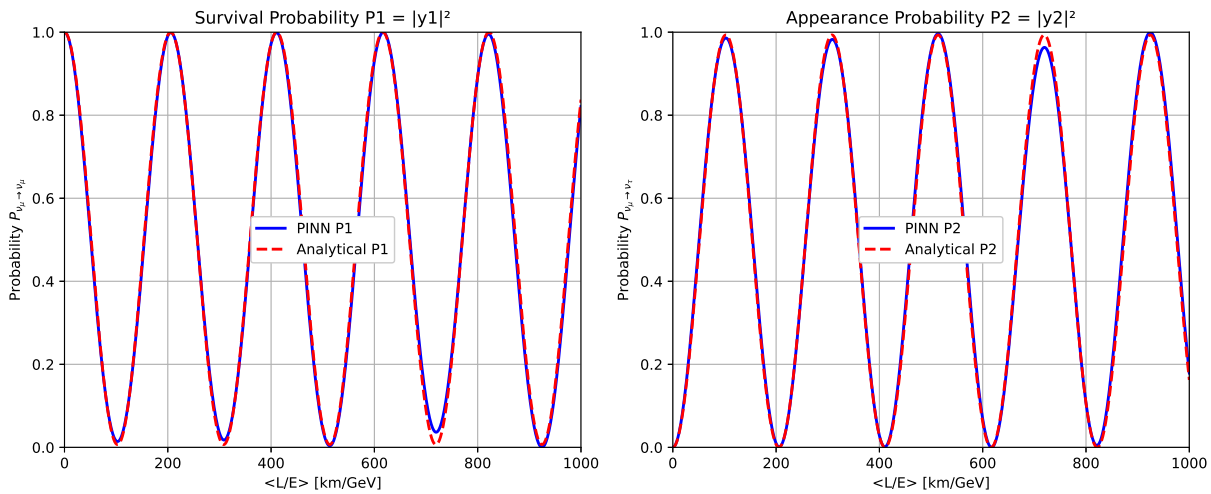


FIG. 6. Survival and Appearance Probability of Atmospheric neutrino in constant matter case

No. SR/FST/ET-I/2022/1079], and a matching grant from VIT University. The authors are grateful to DST-FIST and VIT management for their financial support and the resources provided for this work. We would also like to express our sincere gratitude to Dr. Suprabh

Prakash, whose research expertise in Neutrino Physics and Phenomenology was instrumental to this work. We are deeply grateful for his invaluable technical support and for the guidance that helped us gain a better understanding of the complex concepts involved in this research.

[1] Y. Fukuda, T. Hayakawa, E. Ichihara, K. Inoue, K. Ishihara, H. Ishino, Y. Itow, T. Kajita, J. Kameda, S. Kasuga, K. Kobayashi, Y. Kobayashi, Y. Koshio, M. Miura, M. Nakahata, S. Nakayama, A. Okada, K. Okumura, N. Sakurai, M. Shiozawa, Y. Suzuki, Y. Takeuchi, Y. Totsuka, S. Yamada, M. Earl, A. Habig, E. Kearns, M. D. Messier, K. Scholberg, J. L. Stone, L. R. Sulak, C. W. Walter, M. Goldhaber, T. Barszczak, D. Casper, W. Gajewski, P. G. Halverson, J. Hsu, W. R. Kropp, L. R. Price, F. Reines, M. Smy, H. W. Sobel, M. R. Vagins, K. S. Ganezer, W. E. Keig, R. W. Ellsworth, S. Tasaka, J. W. Flanagan, A. Kibayashi, J. G. Learned, S. Matsuno, V. J. Stenger, D. Takemori, T. Ishii, J. Kanzaki, T. Kobayashi, S. Mine, K. Nakamura, K. Nishikawa, Y. Oyama, A. Sakai, M. Sakuda, O. Sasaki, S. Echigo, M. Kohama, A. T. Suzuki, T. J. Haines, E. Blaufuss, B. K. Kim, R. Sanford, R. Svoboda, M. L. Chen, Z. Conner, J. A. Goodman, G. W. Sullivan, J. Hill, C. K. Jung, K. Martens, C. Mauger, C. McGrew, E. Sharkey, B. Viren, C. Yanagisawa, W. Doki, K. Miyano, H. Okazawa, C. Saji, M. Takahata, Y. Nagashima, M. Takita, T. Yamaguchi, M. Yoshida, S. B. Kim, M. Etoh, K. Fujita, A. Hasegawa, T. Hasegawa, S. Hatakeyama, T. Iwamoto, M. Koga, T. Maruyama, H. Ogawa, J. Shirai, A. Suzuki, F. Tsushima, M. Koshihara, M. Nemoto, K. Nishijima, T. Futagami, Y. Hayato, Y. Kanaya, K. Kaneyuki, Y. Watanabe, D. Kielczewska, R. A. Doyle, J. S. George, A. L. Stachyra, L. L. Wai, R. J. Wilkes, and K. K. Young (Super-Kamiokande Collaboration), Evidence for oscillation of atmospheric neutrinos, *Phys. Rev. Lett.* **81**, 1562 (1998).

[2] Q. R. Ahmad, R. C. Allen, T. C. Andersen, J. D. Anglin, J. C. Barton, E. W. Beier, M. Bercovitch, J. Bigu, S. D. Biller, R. A. Black, I. Blevis, R. J. Boardman, J. Boger, E. Bonvin, M. G. Boulay, M. G. Bowler, T. J. Bowles, S. J. Brice, M. C. Browne, T. V. Bullard, G. Bühler, J. Cameron, Y. D. Chan, H. H. Chen, M. Chen, X. Chen, B. T. Cleveland, E. T. H. Clifford, J. H. M. Cowan, D. F. Cowen, G. A. Cox, X. Dai, F. Dalnoki-Veress, W. F. Davidson, P. J. Doe, G. Doucas, M. R. Dragowsky, C. A. Duba, F. A. Duncan, M. Dunford, J. A. Dunmore, E. D. Earle, S. R. Elliott, H. C. Evans, G. T. Ewan, J. Farine, H. Fergani, A. P. Ferraris, R. J. Ford, J. A. Formaggio, M. M. Fowler, K. Frame, E. D. Frank, W. Frati, N. Gagnon, J. V. Germani, S. Gil, K. Graham, D. R. Grant, R. L. Hahn, A. L. Hallin, E. D. Hallman, A. S. Hamer, A. A. Hamian, W. B. Handler, R. U. Haq, C. K. Hargrove, P. J. Harvey, R. Hazama, K. M. Heeger, W. J. Heintzelman, J. Heise, R. L. Helmer, J. D. Hepburn, H. Heron, J. Hewett, A. Hime, M. Howe, J. G. Hykawy, M. C. P. Isaac, P. Jagam, N. A. Jelley, C. Jillings, G. Jonkmans, K. Kazkaz, P. T. Keener, J. R. Klein, A. B. Knox, R. J. Komar, R. Kouzes, T. Kutter, C. C. M. Kyba, J. Law, I. T. Lawson, M. Lay, H. W. Lee, K. T. Lesko, J. R. Leslie, I. Levine, W. Locke, S. Luoma, J. Lyon, S. Majerus, H. B. Mak, J. Maneira, J. Manor, A. D. Marino, N. McCauley, A. B. McDonald, D. S. McDonald, K. McFarlane, G. McGregor, R. Meijer Drees, C. Mifflin, G. G. Miller, G. Milton, B. A. Moffat, M. Moorhead, C. W. Nally, M. S. Neubauer, F. M. Newcomer, H. S. Ng, A. J. Noble, E. B. Norman, V. M. Novikov, M. O'Neill, C. E. Okada, R. W.

- Ollerhead, M. Omori, J. L. Orrell, S. M. Oser, A. W. P. Poon, T. J. Radcliffe, A. Roberge, B. C. Robertson, R. G. H. Robertson, S. S. E. Rosendahl, J. K. Rowley, V. L. Rusu, E. Saettler, K. K. Schaffer, M. H. Schwendener, A. Schülke, H. Seifert, M. Shatkay, J. J. Simpson, C. J. Sims, D. Sinclair, P. Skensved, A. R. Smith, M. W. E. Smith, T. Spreitzer, N. Starinsky, T. D. Steiger, R. G. Stokstad, L. C. Stonehill, R. S. Storey, B. Sur, R. Tafirout, N. Tagg, N. W. Tanner, R. K. Taplin, M. Thorman, P. M. Thornewell, P. T. Trent, Y. I. Tserkovnyak, R. Van Berg, R. G. Van de Water, C. J. Virtue, C. E. Waltham, J.-X. Wang, D. L. Wark, N. West, J. B. Wilhelm, J. F. Wilkerson, J. R. Wilson, P. Wittich, J. M. Wouters, and M. Yeh (SNO Collaboration), Direct evidence for neutrino flavor transformation from neutral-current interactions in the sudbury neutrino observatory, *Phys. Rev. Lett.* **89**, 011301 (2002).
- [3] C. Giunti and C. W. Kim, *Fundamentals of Neutrino Physics and Astrophysics* (Oxford University Press, 2007).
- [4] K. Eguchi, S. Enomoto, K. Furuno, J. Goldman, H. Hanada, H. Ikeda, K. Ikeda, K. Inoue, K. Ishihara, W. Itoh, T. Iwamoto, T. Kawaguchi, T. Kawashima, H. Kinoshita, Y. Kishimoto, M. Koga, Y. Koseki, T. Maeda, T. Mitsui, M. Motoki, K. Nakajima, M. Nakajima, T. Nakajima, H. Ogawa, K. Owada, T. Sakabe, I. Shimizu, J. Shirai, F. Suekane, A. Suzuki, K. Tada, O. Tajima, T. Takayama, K. Tamae, H. Watanabe, J. Busenitz, Z. Djurcic, K. McKinny, D.-M. Mei, A. Piepke, E. Yakushev, B. E. Berger, Y. D. Chan, M. P. Decowski, D. A. Dwyer, S. J. Freedman, Y. Fu, B. K. Fujikawa, K. M. Heeger, K. T. Lesko, K.-B. Luk, H. Murayama, D. R. Nygren, C. E. Okada, A. W. P. Poon, H. M. Steiner, L. A. Winslow, G. A. Horton-Smith, R. D. McKeown, J. Ritter, B. Tipton, P. Vogel, C. E. Lane, T. Miletic, P. W. Gorham, G. Guillian, J. G. Learned, J. Maricic, S. Matsumo, S. Pakvasa, S. Dazeley, S. Hatakeyama, M. Murakami, R. C. Svoboda, B. D. Dieterle, M. DiMauro, J. Detwiler, G. Gratta, K. Ishii, N. Tolich, Y. Uchida, M. Batygov, W. Bugg, H. Cohn, Y. Efremenko, Y. Kamyshev, A. Kozlov, Y. Nakamura, L. D. Braeckeleer, C. R. Gould, H. J. Karwowski, D. M. Markoff, J. A. Messimore, K. Nakamura, R. M. Rohm, W. Tornow, A. R. Young, and Y.-F. Wang (KamLAND Collaboration), First results from kamland: Evidence for reactor antineutrino disappearance, *Phys. Rev. Lett.* **90**, 021802 (2003).
- [5] K. Abe, N. Abgrall, Y. Ajima, H. Aihara, J. B. Albert, C. Andreopoulos, B. Andrieu, S. Aoki, O. Araoka, J. Argyriades, A. Ariga, T. Ariga, S. Assylbekov, D. Autiero, A. Badertscher, M. Barbi, G. J. Barker, G. Barr, M. Bass, F. Bay, S. Bentham, V. Berardi, B. E. Berger, I. Bertram, M. Besnier, J. Beucher, D. Beznosko, S. Bhadra, F. d. M. Blaszczyk, A. Blondel, C. Bojchko, J. Bouchez, S. B. Boyd, A. Bravar, C. Bronner, D. G. Brook-Robert, N. Buchanan, H. Budd, D. Calvet, S. L. Cartwright, A. Carver, R. Castillo, M. G. Catanesi, A. Cazes, A. Cervera, C. Chavez, S. Choi, G. Christodoulou, J. Coleman, W. Coleman, G. Collazuol, K. Connolly, A. Curioni, A. Dabrowska, I. Danko, R. Das, G. S. Davies, S. Davis, M. Day, G. De Rosa, J. P. A. M. de André, P. de Perio, A. Delbart, C. Densham, F. Di Lodovico, S. Di Luise, P. Dinh Tran, J. Dobson, U. Dore, O. Drapier, F. Dufour, J. Dumarchez, S. Dytman, M. Dziewiecki, M. Dziomba, S. Emery, A. Ereditato, L. Escudero, L. S. Esposito, M. Fechner, A. Ferrero, A. J. Finch, E. Frank, Y. Fujii, Y. Fukuda, V. Galymov, F. C. Gannaway, A. Gaudin, A. Gendotti, M. A. George, S. Giffin, C. Giganti, K. Gilje, T. Golan, M. Goldhaber, J. J. Gomez-Cadenas, M. Gonin, N. Grant, A. Grant, P. Gumplinger, P. Guzowski, A. Haesler, M. D. Haigh, K. Hamano, C. Hansen, D. Hansen, T. Hara, P. F. Harrison, B. Hartfiel, M. Hartz, T. Haruyama, T. Hasegawa, N. C. Hastings, S. Hastings, A. Hatzikoutelis, K. Hayashi, Y. Hayato, C. Hearty, R. L. Helmer, R. Henderson, N. Higashi, J. Hignight, E. Hirose, J. Holeczek, S. Horikawa, A. Hyndman, A. K. Ichikawa, K. Ieki, M. Ieva, M. Iida, M. Ikeda, J. Ilic, J. Imber, T. Ishida, C. Ishihara, T. Ishii, S. J. Ives, M. Iwasaki, K. Iyogi, A. Izmaylov, B. Jamieson, R. A. Johnson, K. K. Joo, G. V. Jovermanas, C. K. Jung, H. Kaji, T. Kajita, H. Kakuno, J. Kameda, K. Kaneyuki, D. Karlen, K. Kasami, I. Kato, E. Kearns, M. Khabibullin, F. Khanam, A. Khotjantsev, D. Kielczewska, T. Kikawa, J. Kim, J. Y. Kim, S. B. Kim, N. Kimura, B. Kirby, J. Kisiel, P. Kitching, T. Kobayashi, G. Kogan, S. Koike, A. Konaka, L. L. Kormos, A. Korzenev, K. Koseki, Y. Koshio, Y. Kouzuma, K. Kowalik, V. Kravtsov, I. Kreslo, W. Kropp, H. Kubo, Y. Kudenko, N. Kulkarni, R. Kurjata, T. Kutter, J. Lagoda, K. Laihem, M. Laveder, K. P. Lee, P. T. Le, J. M. Levy, C. Licciardi, I. T. Lim, T. Lindner, R. P. Litchfield, M. Litos, A. Longhin, G. D. Lopez, P. F. Loverre, L. Ludovici, T. Lux, M. Macaire, K. Mahn, Y. Makida, M. Malek, S. Manly, A. Marchionni, A. D. Marino, J. Marteau, J. F. Martin, T. Maruyama, T. Maryon, J. Marzec, P. Masliha, E. L. Mathie, C. Matsumura, K. Matsuoaka, V. Matveev, K. Mavrokoridis, E. Mazzucato, N. McCauley, K. S. McFarland, C. McGrew, T. McLachlan, M. Messina, W. Metcalf, C. Metelko, M. Mezzetto, P. Mijakowski, C. A. Miller, A. Minamino, O. Mineev, S. Mine, A. D. Missert, G. Mituka, M. Miura, K. Mizouchi, L. Monfregola, F. Moreau, B. Morgan, S. Moriyama, A. Muir, A. Murakami, M. Murdoch, S. Murphy, J. Myslik, T. Nakadaira, M. Nakahata, T. Nakai, K. Nakajima, T. Nakamoto, K. Nakamura, S. Nakayama, T. Nakaya, D. Naples, M. L. Navin, B. Nelson, T. C. Nicholls, K. Nishikawa, H. Nishino, J. A. Nowak, M. Noy, Y. Obayashi, T. Ogitsu, H. Ohhata, T. Okamura, K. Okumura, T. Okusawa, S. M. Oser, M. Otani, R. A. Owen, Y. Oyama, T. Ozaki, M. Y. Pac, V. Paladino, V. Paolone, P. Paul, D. Payne, G. F. Pearce, J. D. Perkin, V. Pettinacci, F. Pierre, E. Poplawska, B. Popov, M. Posiadala, J.-M. Poutissou, R. Poutissou, P. Przewlocki, W. Qian, J. L. Raaf, E. Radicioni, P. N. Ratoff, T. M. Raufer, M. Ravonel, M. Raymond, F. Retiere, A. Robert, P. A. Rodrigues, E. Rondio, J. M. Roney, B. Rossi, S. Roth, A. Rubbia, D. Ruterbories, S. Sabouri, R. Sacco, K. Sakashita, F. Sánchez, A. Sarraf, K. Sasaki, K. Scholberg, J. Schwehr, M. Scott, D. I. Scully, Y. Seiya, T. Sekiguchi, H. Sekiya, M. Shibata, Y. Shimizu, M. Shiozawa, S. Short, M. Siyad, R. J. Smith, M. Smy, J. T. Sobczyk, H. Sobel, M. Sorel, A. Stahl, P. Stamoulis, J. Steinmann, B. Still, J. Stone, C. Strabel, L. R. Sulak, R. Sulej, P. Sutcliffe, A. Suzuki, K. Suzuki, S. Suzuki, S. Y. Suzuki, Y. Suzuki, Y. Suzuki, T. Szeplowski, M. Szeptycka, R. Tacik, M. Tada, S. Taka-

- hashi, A. Takeda, Y. Takenaga, Y. Takeuchi, K. Tanaka, H. A. Tanaka, M. Tanaka, M. M. Tanaka, N. Tanimoto, K. Tashiro, I. Taylor, A. Terashima, D. Terhorst, R. Terri, L. F. Thompson, A. Thorley, W. Toki, T. Tomaru, Y. Totsuka, C. Touramanis, T. Tsukamoto, M. Tzanov, Y. Uchida, K. Ueno, A. Vacheret, M. Vagins, G. Vasseur, T. Wachala, J. J. Walding, A. V. Waldron, C. W. Walter, P. J. Wanderer, J. Wang, M. A. Ward, G. P. Ward, D. Wark, M. O. Wascko, A. Weber, R. Wendell, N. West, L. H. Whitehead, G. Wikström, R. J. Wilkes, M. J. Wilking, J. R. Wilson, R. J. Wilson, T. Wongjirad, S. Yamada, Y. Yamada, A. Yamamoto, K. Yamamoto, Y. Yamanoi, H. Yamaoka, C. Yanagisawa, T. Yano, S. Yen, N. Yershov, M. Yokoyama, A. Zalewska, J. Zalipska, L. Zambelli, K. Zaremba, M. Ziemicki, E. D. Zimmerman, M. Zito, and J. Żmuda (T2K Collaboration), Indication of electron neutrino appearance from an accelerator-produced off-axis muon neutrino beam, *Phys. Rev. Lett.* **107**, 041801 (2011).
- [6] F. P. An, J. Z. Bai, A. B. Balantekin, H. R. Band, D. Beavis, W. Beriguete, M. Bishai, S. Blyth, K. Boddy, R. L. Brown, B. Cai, G. F. Cao, J. Cao, R. Carr, W. T. Chan, J. F. Chang, Y. Chang, C. Chasman, H. S. Chen, H. Y. Chen, S. J. Chen, S. M. Chen, X. C. Chen, X. H. Chen, X. S. Chen, Y. Chen, Y. X. Chen, J. J. Chervinka, M. C. Chu, J. P. Cummings, Z. Y. Deng, Y. Y. Ding, M. V. Diwan, L. Dong, E. Draeger, X. F. Du, D. A. Dwyer, W. R. Edwards, S. R. Ely, S. D. Fang, J. Y. Fu, Z. W. Fu, L. Q. Ge, V. Ghazikhanian, R. L. Gill, J. Goett, M. Gonchar, G. H. Gong, H. Gong, Y. A. Gornushkin, L. S. Greenler, W. Q. Gu, M. Y. Guan, X. H. Guo, R. W. Hackenburg, R. L. Hahn, S. Hans, M. He, Q. He, W. S. He, K. M. Heeger, Y. K. Heng, P. Hinrichs, T. H. Ho, Y. K. Hor, Y. B. Hsiung, B. Z. Hu, T. Hu, T. Hu, H. X. Huang, H. Z. Huang, P. W. Huang, X. Huang, X. T. Huang, P. Huber, Z. Isvan, D. E. Jaffe, S. Jetter, X. L. Ji, X. P. Ji, H. J. Jiang, W. Q. Jiang, J. B. Jiao, R. A. Johnson, L. Kang, S. H. Kettell, M. Kramer, K. K. Kwan, M. W. Kwok, T. Kwok, C. Y. Lai, W. C. Lai, W. H. Lai, K. Lau, L. Lebanowski, J. Lee, M. K. P. Lee, R. Leitner, J. K. C. Leung, K. Y. Leung, C. A. Lewis, B. Li, F. Li, G. S. Li, J. Li, Q. J. Li, S. F. Li, W. D. Li, X. B. Li, X. N. Li, X. Q. Li, Y. Li, Z. B. Li, H. Liang, J. Liang, C. J. Lin, G. L. Lin, S. K. Lin, S. X. Lin, Y. C. Lin, J. J. Ling, J. M. Link, L. Littenberg, B. R. Littlejohn, B. J. Liu, C. Liu, D. W. Liu, H. Liu, J. C. Liu, J. L. Liu, S. Liu, X. Liu, Y. B. Liu, C. Lu, H. Q. Lu, A. Luk, K. B. Luk, T. Luo, X. L. Luo, L. H. Ma, Q. M. Ma, X. B. Ma, X. Y. Ma, Y. Q. Ma, B. Mayes, K. T. McDonald, M. C. McFarlane, R. D. McKeown, Y. Meng, D. Mohapatra, J. E. Morgan, Y. Nakajima, J. Napolitano, D. Naumov, I. Nemchenok, C. Newsom, H. Y. Ngai, W. K. Ngai, Y. B. Nie, Z. Ning, J. P. Ochoa-Ricoux, D. Oh, A. Olshevski, A. Pagac, S. Patton, C. Pearson, V. Pec, J. C. Peng, L. E. Pilonen, L. Pinsky, C. S. J. Pun, F. Z. Qi, M. Qi, X. Qian, N. Raper, R. Rosero, B. Roskovec, X. C. Ruan, B. Seilhan, B. B. Shao, K. Shih, H. Steiner, P. Stoler, G. X. Sun, J. L. Sun, Y. H. Tam, H. K. Tanaka, X. Tang, H. Themann, Y. Torun, S. Trentalange, O. Tsai, K. V. Tsang, R. H. M. Tsang, C. Tull, B. Viren, S. Virostek, V. Vorobel, C. H. Wang, L. S. Wang, L. Y. Wang, L. Z. Wang, M. Wang, N. Y. Wang, R. G. Wang, T. Wang, W. Wang, X. Wang, X. Wang, Y. F. Wang, Z. Wang, Z. Wang, Z. M. Wang, D. M. Webber, Y. D. Wei, L. J. Wen, D. L. Wenman, K. Whisnant, C. G. White, L. Whitehead, C. A. Whitten, J. Wilhelmi, T. Wise, H. C. Wong, H. L. H. Wong, J. Wong, E. T. Worcester, F. F. Wu, Q. Wu, D. M. Xia, S. T. Xiang, Q. Xiao, Z. Z. Xing, G. Xu, J. Xu, J. Xu, J. L. Xu, W. Xu, Y. Xu, T. Xue, C. G. Yang, L. Yang, M. Ye, M. Yeh, Y. S. Yeh, K. Yip, B. L. Young, Z. Y. Yu, L. Zhan, C. Zhang, F. H. Zhang, J. W. Zhang, Q. M. Zhang, K. Zhang, Q. X. Zhang, S. H. Zhang, Y. C. Zhang, Y. H. Zhang, Y. X. Zhang, Z. J. Zhang, Z. P. Zhang, Z. Y. Zhang, J. Zhao, Q. W. Zhao, Y. B. Zhao, L. Zheng, W. L. Zhong, L. Zhou, Z. Y. Zhou, H. L. Zhuang, and J. H. Zou, Observation of electron-antineutrino disappearance at daya bay, *Phys. Rev. Lett.* **108**, 171803 (2012).
- [7] P. A. Zyla *et al.* (Particle Data Group), Review of Particle Physics, *PTEP* **2020**, 083C01 (2020).
- [8] I. Esteban, M. C. Gonzalez-Garcia, M. Maltoni, T. Schwetz, and A. Zhou, The fate of hints: updated global analysis of three-flavor neutrino oscillations, *JHEP* **09**, 178, arXiv:2007.14792 [hep-ph].
- [9] P. F. de Salas, D. V. Forero, S. Gariazzo, P. Martínez-Miravé, O. Mena, C. A. Ternes, M. Törtola, and J. W. F. Valle, 2020 global reassessment of the neutrino oscillation picture, *Journal of High Energy Physics* **2021**, 71 (2021), arXiv:2006.11237 [hep-ph].
- [10] T. A. Mueller, D. Lhuillier, M. Fallot, A. Letourneau, S. Cormon, M. Fechner, L. Giot, T. Lasserre, J. Martino, G. Mention, A. Porta, and F. Yermia, Improved predictions of reactor antineutrino spectra, *Phys. Rev. C* **83**, 054615 (2011).
- [11] J. K. Ahn, S. Chebotaryov, J. H. Choi, S. Choi, W. Choi, Y. Choi, H. I. Jang, J. S. Jang, E. J. Jeon, I. S. Jeong, K. K. Joo, B. R. Kim, B. C. Kim, H. S. Kim, J. Y. Kim, S. B. Kim, S. H. Kim, S. Y. Kim, W. Kim, Y. D. Kim, J. Lee, J. K. Lee, I. T. Lim, K. J. Ma, M. Y. Pac, I. G. Park, J. S. Park, K. S. Park, J. W. Shin, K. Siyeon, B. S. Yang, I. S. Yeo, S. H. Yi, and I. Yu (RENO Collaboration), Observation of reactor electron antineutrinos disappearance in the reno experiment, *Phys. Rev. Lett.* **108**, 191802 (2012).
- [12] F. P. An, A. B. Balantekin, H. R. Band, M. Bishai, S. Blyth, I. Butorov, D. Cao, G. F. Cao, J. Cao, W. R. Cen, Y. L. Chan, J. F. Chang, L. C. Chang, Y. Chang, H. S. Chen, Q. Y. Chen, S. M. Chen, Y. X. Chen, Y. Chen, J. H. Cheng, J. Cheng, Y. P. Cheng, J. J. Chervinka, M. C. Chu, J. P. Cummings, J. de Arcos, Z. Y. Deng, X. F. Ding, Y. Y. Ding, M. V. Diwan, J. Dove, E. Draeger, D. A. Dwyer, W. R. Edwards, S. R. Ely, R. Gill, M. Gonchar, G. H. Gong, H. Gong, M. Grassi, W. Q. Gu, M. Y. Guan, L. Guo, X. H. Guo, R. W. Hackenburg, R. Han, S. Hans, M. He, K. M. Heeger, Y. K. Heng, A. Higuera, Y. K. Hor, Y. B. Hsiung, B. Z. Hu, L. M. Hu, L. J. Hu, T. Hu, W. Hu, E. C. Huang, H. X. Huang, X. T. Huang, P. Huber, G. Hussain, D. E. Jaffe, P. Jaffke, K. L. Jen, S. Jetter, X. P. Ji, X. L. Ji, J. B. Jiao, R. A. Johnson, L. Kang, S. H. Kettell, S. Kohn, M. Kramer, K. K. Kwan, M. W. Kwok, T. Kwok, T. J. Langford, K. Lau, L. Lebanowski, J. Lee, R. T. Lei, R. Leitner, K. Y. Leung, J. K. C. Leung, C. A. Lewis, D. J. Li, F. Li, G. S. Li, Q. J. Li, S. C. Li, W. D. Li, X. N. Li, X. Q. Li, Y. F. Li, Z. B. Li, H. Liang, C. J. Lin, G. L. Lin, P. Y. Lin, S. K. Lin, J. J. Ling, J. M. Link, L. Littenberg, B. R. Littlejohn, D. W. Liu, H. Liu, J. L. Liu, J. C. Liu, S. S. Liu, C. Lu, H. Q. Lu, J. S. Lu,

- K. B. Luk, Q. M. Ma, X. Y. Ma, X. B. Ma, Y. Q. Ma, D. A. Martinez Caicedo, K. T. McDonald, R. D. McKeown, Y. Meng, I. Mitchell, J. Monari Kebwaro, Y. Nakajima, J. Napolitano, D. Naumov, E. Naumova, H. Y. Ngai, Z. Ning, J. P. Ochoa-Ricoux, A. Olshevski, H.-R. Pan, J. Park, S. Patton, V. Pec, J. C. Peng, L. E. Piilonen, L. Pinsky, C. S. J. Pun, F. Z. Qi, M. Qi, X. Qian, N. Raper, B. Ren, J. Ren, R. Rosero, B. Roskovec, X. C. Ruan, B. B. Shao, H. Steiner, G. X. Sun, J. L. Sun, W. Tang, D. Taychenachev, K. V. Tsang, C. E. Tull, Y. C. Tung, N. Viaux, B. Viren, V. Vorobel, C. H. Wang, M. Wang, N. Y. Wang, R. G. Wang, W. Wang, W. W. Wang, X. Wang, Y. F. Wang, Z. Wang, Z. Wang, Z. M. Wang, H. Y. Wei, L. J. Wen, K. Whisnant, C. G. White, L. Whitehead, T. Wise, H. L. H. Wong, S. C. F. Wong, E. Worcester, Q. Wu, D. M. Xia, J. K. Xia, X. Xia, Z. Z. Xing, J. Y. Xu, J. L. Xu, J. Xu, Y. Xu, T. Xue, J. Yan, C. G. Yang, L. Yang, M. S. Yang, M. T. Yang, M. Ye, M. Yeh, B. L. Young, G. Y. Yu, Z. Y. Yu, S. L. Zang, L. Zhan, C. Zhang, H. H. Zhang, J. W. Zhang, Q. M. Zhang, Y. M. Zhang, Y. X. Zhang, Y. M. Zhang, Z. J. Zhang, Z. Y. Zhang, Z. P. Zhang, J. Zhao, Q. W. Zhao, Y. F. Zhao, Y. B. Zhao, L. Zheng, W. L. Zhong, L. Zhou, N. Zhou, H. L. Zhuang, and J. H. Zou (Daya Bay Collaboration), Measurement of the reactor antineutrino flux and spectrum at daya bay, *Phys. Rev. Lett.* **116**, 061801 (2016).
- [13] M. C. Gonzalez-Garcia, M. Maltoni, J. Salvado, and T. Schwetz, Global fit to three neutrino mixing: critical look at present precision, *JHEP* **12**, 123, arXiv:1209.3023 [hep-ph].
- [14] T. K. Gaisser and M. Honda, Flux of atmospheric neutrinos, *Ann. Rev. Nucl. Part. Sci.* **52**, 153 (2002), arXiv:hep-ph/0203272.
- [15] T. KAJITA, Atmospheric neutrinos and discovery of neutrino oscillations, *Proceedings of the Japan Academy, Series B* **86**, 303 (2010).
- [16] E. K. Akhmedov, Neutrino Physics, in *Particle Physics*, edited by G. Senjanović and A. Y. Smirnov (2000) p. 103, arXiv:hep-ph/0001264 [hep-ph].
- [17] K. Abe, C. Bronner, Y. Haga, Y. Hayato, M. Ikeda, K. Iyogi, J. Kameda, Y. Kato, Y. Kishimoto, L. Marti, M. Miura, S. Moriyama, M. Nakahata, T. Nakajima, Y. Nakano, S. Nakayama, Y. Okajima, A. Orii, G. Pronost, H. Sekiya, M. Shiozawa, Y. Sonoda, A. Takeda, A. Takenaka, H. Tanaka, S. Tasaka, T. Tomura, R. Akutsu, T. Irvine, T. Kajita, I. Kametani, K. Kaneyuki, Y. Nishimura, K. Okumura, E. Richard, K. M. Tsui, L. Labarga, P. Fernandez, F. d. M. Blaszczyk, J. Gustafson, C. Kachulis, E. Kearns, J. L. Raaf, J. L. Stone, L. R. Sulak, S. Berkman, S. Toyabayama, M. Goldhaber, G. Carminati, M. Elnimr, W. R. Kropp, S. Mine, S. Locke, A. Renshaw, M. B. Smy, H. W. Sobel, V. Takhistov, P. Weatherly, K. S. Ganezer, B. L. Hartfiel, J. Hill, N. Hong, J. Y. Kim, I. T. Lim, R. G. Park, T. Akiri, A. Himmel, Z. Li, E. O'Sullivan, K. Scholberg, C. W. Walter, T. Wongji-rad, T. Ishizuka, T. Nakamura, J. S. Jang, K. Choi, J. G. Learned, S. Matsuno, S. N. Smith, J. Amey, R. P. Litchfield, W. Y. Ma, Y. Uchida, M. O. Wascko, S. Cao, M. Friend, T. Hasegawa, T. Ishida, T. Ishii, T. Kobayashi, T. Nakadaira, K. Nakamura, Y. Oyama, K. Sakashita, T. Sekiguchi, T. Tsukamoto, K. Abe, M. Hasegawa, A. T. Suzuki, Y. Takeuchi, T. Yano, T. Hayashino, S. Hirota, K. Huang, K. Ieki, M. Jiang, T. Kikawa, K. Nakamura, T. Nakaya, N. D. Patel, K. Suzuki, S. Takahashi, R. A. Wendell, L. H. V. Anthony, N. McCauley, A. Pritchard, Y. Fukuda, Y. Itow, G. Mitsuka, M. Murase, F. Muto, T. Suzuki, P. Mijakowski, K. Frankiewicz, J. Hignight, J. Imber, C. K. Jung, X. Li, J. L. Palomino, G. Santucci, C. Vilela, M. J. Wilking, C. Yanagisawa, S. Ito, D. Fukuda, H. Ishino, T. Kayano, A. Kibayashi, Y. Koshio, T. Mori, H. Nagata, M. Sakuda, C. Xu, Y. Kuno, D. Wark, F. Di Lodovico, B. Richards, R. Tacik, S. B. Kim, A. Cole, L. Thompson, H. Okazawa, Y. Choi, K. Ito, K. Nishijima, M. Koshihara, Y. Totsuka, Y. Suda, M. Yokoyama, R. G. Calland, M. Hartz, K. Martens, B. Quilain, C. Simpson, Y. Suzuki, M. R. Vagins, D. Hamabe, M. Kuze, T. Yoshida, M. Ishitsuka, J. F. Martin, C. M. Nantais, P. de Perio, H. A. Tanaka, A. Konaka, S. Chen, L. Wan, Y. Zhang, R. J. Wilkes, and A. Minamino (Super-Kamiokande Collaboration), Atmospheric neutrino oscillation analysis with external constraints in super-kamiokande i-iv, *Phys. Rev. D* **97**, 072001 (2018).
- [18] M. A. Acero, P. Adamson, L. Aliaga, T. Alion, V. Alkhalverdian, S. Altakarli, N. Anfimov, A. Antoshkin, A. Aurisano, A. Back, C. Backhouse, M. Baird, N. Balashov, P. Baldi, B. A. Bambah, S. Bashar, K. Bays, S. Bending, R. Bernstein, V. Bhatnagar, B. Bhuyan, J. Bian, T. Blackburn, J. Blair, A. C. Booth, P. Bour, C. Bromberg, N. Buchanan, A. Butkevich, S. Calvez, M. Campbell, T. J. Carroll, E. Catano-Mur, A. Cedenno, S. Childress, B. C. Choudhary, B. Chowdhury, T. E. Coan, M. Colo, J. Cooper, L. Corwin, L. Cremonesi, G. S. Davies, P. F. Derwent, P. Ding, Z. Djurcic, D. Doyle, E. C. Dukes, H. Duyang, S. Edayath, R. Ehrlich, M. Elkins, G. J. Feldman, P. Filip, W. Flanagan, M. J. Frank, H. R. Gallagher, R. Gandrajula, F. Gao, S. Germani, A. Giri, R. A. Gomes, M. C. Goodman, V. Grichine, M. Groh, R. Group, B. Guo, A. Habig, F. Hakl, J. Hartnell, R. Hatcher, A. Hatzikoutelis, K. Heller, J. Hewes, A. Himmel, A. Holin, B. Howard, J. Huang, J. Hylen, F. Jediny, C. Johnson, M. Judah, I. Kakorin, D. Kalra, D. M. Kaplan, R. Keloth, O. Klimov, L. W. Koerner, L. Kolupaeva, S. Kotelnikov, I. Kourbanis, A. Kreymer, C. Kulenberg, A. Kumar, C. D. Kuruppu, V. Kus, T. Lackey, K. Lang, S. Lin, M. Lokajicek, J. Lozier, S. Luchuk, K. Maan, S. Magill, W. A. Mann, M. L. Marshak, M. Martinez-Casales, V. Matveev, D. P. Méndez, M. D. Messier, H. Meyer, T. Miao, W. H. Miller, S. R. Mishra, A. Mislivec, R. Mohanta, A. Moren, L. Muallem, M. Muether, S. Mufson, K. Mulder, R. Murphy, J. Musser, D. Naples, N. Nayak, J. K. Nelson, R. Nichol, G. Nikseresht, E. Niner, A. Norman, T. Nosek, A. Olshevskiy, T. Olson, J. Paley, R. B. Patterson, G. Pawloski, D. Pershey, O. Petrova, R. Petti, D. D. Phan, R. K. Plunkett, B. Potukuchi, C. Principato, F. Psihas, A. Radovic, V. Raj, R. A. Rameika, B. Rebel, P. Rojas, V. Ryabov, O. Samoylov, M. C. Sanchez, S. Sánchez Falero, I. S. Seong, P. Shanahan, A. Sheshukov, P. Singh, V. Singh, E. Smith, J. Smolik, P. Snopok, N. Solomey, E. Song, A. Sousa, K. Sous-truznik, M. Strait, L. Suter, A. Sutton, R. L. Talaga, B. Tapia Oregui, P. Tas, R. B. Thayyullathil, J. Thomas, E. Tiras, D. Torbunov, J. Tripathi, A. Tsaris, Y. Torun, J. Urheim, P. Vahle, J. Vasel, L. Vinton, P. Vokac, T. Vrba, M. Wallbank, B. Wang, T. K. Warburton,

- M. Wetstein, M. While, D. Whittington, S. G. Wojcicki, J. Wolcott, N. Yadav, A. Yallappa Dombara, K. Yonehara, S. Yu, S. Zadorozhnyy, J. Zalesak, B. Zamorano, and R. Zwaska (NOvA Collaboration), First measurement of neutrino oscillation parameters using neutrinos and antineutrinos by nova, *Phys. Rev. Lett.* **123**, 151803 (2019).
- [19] W. H. Press, S. A. Teukolsky, W. T. Vetterling, and B. P. Flannery, *Numerical Recipes: The Art of Scientific Computing* (Cambridge University Press, 2007).
- [20] A. M. Dziewonski and D. L. Anderson, Preliminary reference earth model, *Phys. Earth Planet. Interiors* **25**, 297 (1981).
- [21] J. Kopp, *Phenomenology of Three-Flavour Neutrino Oscillations*, diploma, Technische Universität München, München (2006).
- [22] G. Morales, G. Lehaut, A. Vacheret, F. Jurie, and J. Fadili, Neutrino Oscillation Parameter Estimation Using Structured Hierarchical Transformers, *arXiv e-prints*, [arXiv:2603.22342](https://arxiv.org/abs/2603.22342) (2026), [arXiv:2603.22342](https://arxiv.org/abs/2603.22342) [hep-ph].
- [23] M. Raissi, P. Perdikaris, and G. E. Karniadakis, Physics-informed neural networks: A deep learning framework for solving forward and inverse problems involving nonlinear partial differential equations, *Journal of Computational Physics* **378**, 686 (2019).
- [24] G. Carleo, I. Cirac, K. Cranmer, L. Daudet, M. Schuld, N. Tishby, L. Vogt-Maranto, and L. Zdeborová, Machine learning and the physical sciences, *Reviews of Modern Physics* **91**, 045002 (2019).
- [25] G. Karniadakis, Y. Kevrekidis, L. Lu, P. Perdikaris, S. Wang, and L. Yang, Physics-informed machine learning, *Nature Reviews Physics*, **1** (2021).
- [26] S. Cuomo, V. Schiano di Cola, F. Giampaolo, G. Rozza, M. Raissi, and F. Piccialli, Scientific Machine Learning through Physics-Informed Neural Networks: Where we are and What's next, *arXiv e-prints*, [arXiv:2201.05624](https://arxiv.org/abs/2201.05624) (2022), [arXiv:2201.05624](https://arxiv.org/abs/2201.05624) [cs.LG].
- [27] M. Raissi, A. Yazdani, and G. E. Karniadakis, Hidden fluid mechanics: Learning velocity and pressure fields from flow visualizations, *Science* **367**, 1026 (2020), <https://www.science.org/doi/pdf/10.1126/science.aaw4741>.
- [28] X. Jin, S. Cai, H. Li, and G. E. Karniadakis, NSFnets (Navier-Stokes flow nets): Physics-informed neural networks for the incompressible Navier-Stokes equations, *Journal of Computational Physics* **426**, 109951 (2021), [arXiv:2003.06496](https://arxiv.org/abs/2003.06496) [physics.comp-ph].
- [29] I. E. Lagaris, A. Likas, and D. I. Fotiadis, Artificial Neural Networks for Solving Ordinary and Partial Differential Equations, *arXiv e-prints*, [physics/9705023](https://arxiv.org/abs/physics/9705023) (1997), [arXiv:physics/9705023](https://arxiv.org/abs/physics/9705023) [physics.comp-ph].
- [30] L. Lu, X. Meng, Z. Mao, and G. E. Karniadakis, DeepXDE: A deep learning library for solving differential equations, *arXiv e-prints*, [arXiv:1907.04502](https://arxiv.org/abs/1907.04502) (2019), [arXiv:1907.04502](https://arxiv.org/abs/1907.04502) [cs.LG].
- [31] Z. Maki, M. Nakagawa, and S. Sakata, Remarks on the Unified Model of Elementary Particles, *Progress of Theoretical Physics* **28**, 870 (1962).
- [32] L. Wolfenstein, Neutrino oscillations in matter, *Phys. Rev. D* **17**, 2369 (1978).
- [33] J. N. Bahcall, *NEUTRINO ASTROPHYSICS* (Cambridge University Press, 1989).
- [34] S. Wang, Y. Teng, and P. Perdikaris, Understanding and Mitigating Gradient Flow Pathologies in Physics-Informed Neural Networks, *SIAM Journal on Scientific Computing* **43**, A3055 (2021), [arXiv:2001.04536](https://arxiv.org/abs/2001.04536) [cs.LG].
- [35] D. P. Kingma and J. Ba, Adam: A method for stochastic optimization, *arXiv preprint arXiv:1412.6980* (2014).
- [36] P. Rathore, W. Lei, Z. Frangella, L. Lu, and M. Udell, Challenges in Training PINNs: A Loss Landscape Perspective, *arXiv e-prints*, [arXiv:2402.01868](https://arxiv.org/abs/2402.01868) (2024), [arXiv:2402.01868](https://arxiv.org/abs/2402.01868) [cs.LG].
- [37] A. Hannan Mustajab, H. Lyu, Z. Rizvi, and F. Wuttke, Physics-Informed Neural Networks for High-Frequency and Multi-Scale Problems using Transfer Learning, *arXiv e-prints*, [arXiv:2401.02810](https://arxiv.org/abs/2401.02810) (2024), [arXiv:2401.02810](https://arxiv.org/abs/2401.02810) [cs.LG].
- [38] V. Sitzmann, J. N. P. Martel, A. W. Bergman, D. B. Lindell, and G. Wetzstein, Implicit Neural Representations with Periodic Activation Functions, *arXiv e-prints*, [arXiv:2006.09661](https://arxiv.org/abs/2006.09661) (2020), [arXiv:2006.09661](https://arxiv.org/abs/2006.09661) [cs.CV].
- [39] A. D. Jagtap, K. Kawaguchi, and G. E. Karniadakis, Adaptive activation functions accelerate convergence in deep and physics-informed neural networks, *Journal of Computational Physics* **404**, 109136 (2020), [arXiv:1906.01170](https://arxiv.org/abs/1906.01170) [physics.comp-ph].
- [40] A. Paszke, S. Gross, F. Massa, A. Lerer, J. Bradbury, G. Chanan, T. Killeen, Z. Lin, N. Gimelshein, L. Antiga, *et al.*, Pytorch: An imperative style, high-performance deep learning library, *Advances in neural information processing systems* **32** (2019).
- [41] A. Gunes Baydin, B. A. Pearlmutter, A. Andreyevich Radul, and J. M. Siskind, Automatic differentiation in machine learning: a survey, *arXiv e-prints*, [arXiv:1502.05767](https://arxiv.org/abs/1502.05767) (2015), [arXiv:1502.05767](https://arxiv.org/abs/1502.05767) [cs.SC].